LOW FREQUENCY HIGHLY DIRECTIONAL AIR COUPLED ULTRASOUND SENSOR

Mathew Legg
Massey University, School of Engineering and Advanced Technology, Auckland, New Zealand
email: m.legg@massey.ac.nz

Stuart Bradley
University of Auckland, Physics Department, Auckland, New Zealand

email: s.bradley@auckland.ac.nz

Air coupled ultrasonic transducers are used for non-contact nondestructive evaluation of the properties of materials or structures. To obtain high resolution measurements, these transducers should have highly directional transmit and receive beams and good depth resolution. To achieve this, most transducers operate at ultrasonic frequencies greater than 100 kHz. However, there are many applications were these higher ultrasonic frequencies cannot be used due the high attenuation rates of a material. In these cases, lower ultrasonic frequencies are more suited. However, traditional air coupled transducers have poor resolution at these low frequencies due to wide beam widths and long duration transmit pulses. In this paper, we present a novel air coupled ultrasonic sensor. It has a highly directional transmit and receive beams and improved depth resolution for frequencies from about 25-65 kHz.

Keywords: Ultrasonic, air coupled, transducer, array

1. Introduction

Air coupled ultrasonic transducers are used in a wide range of applications where the properties of a structure or material need to be measured in a non-contact manner. Review papers on air coupled ultrasonic transducers and the materials used to create these are provided in references [1, 2]. These ultrasonic transducers should have highly directional beams and short duration pulses. This is commonly achieved using transducers operating at high ultrasonic frequencies ($>$ 100 kHz). However, there are many mediums for which low ultrasonic frequencies ($<$ 100 kHz) are more suited due to the high attenuation rates. However, transducers operating at these frequencies have wide angle beams and long pulse durations resulting in poor spatial and temporal resolution.

One technique for increasing the spatial resolution is to use multiple transducers in a phased array. While each transducer may have a wide beam angle, placing the transducers in an array may be used to create a focused narrow beam. The minimum spacing between transducer elements should ideally be no more than half of the wavelength (λ) of the signal being transmitted/received otherwise spatial aliasing can occur. This results in multiple beams being formed, instead of a single focused beam. These are sometimes referred to as grating lobes and are generally undesirable.

For high frequency air coupled arrays, techniques such as micromachining are often used to create phased arrays with the required half wavelength minimum spacing between transducer elements [3, 4]. However, for studies using lower ultrasonic frequencies, generally commercially available air coupled transducers have been used in the arrays. These transducers, however, had diameters that were too wide to allow the required $\lambda/2$ spacing to avoid grating lobes from occurring. Blum et al. developed an air coupled transmission array for 50-100 kHz excitation using twenty 32 mm diameter transducers on a concave surface [5]. However, this design showed multiple grating lobes. Konetzke et al. addressed this issue using acoustic wave guides [6]. Tubes were used to funnel the ultrasonic waves from the 10 mm wide transducers to openings which were spaced $\lambda/2 = 4.3$ mm apart. This allowed the $\lambda/2$ spacing to be used and eliminated grating lobes. However, this technique requires wave guides to be constructed and adds thickness to the array. A different technique was used by Korobov et al. [7]. They placing sixty transducers which were 16 mm in diameter into four rings at calculated Fresnel zones and applied anti-phase excitation signals to each zone. This resulted in a fixed focal point 308 mm directly in front of the array. However, a disadvantage of this technique is that the fixed focal point cannot be steered around electronically like a conventional phased array. Kazys et al. developed custom built transducer elements composed of $15 \times 5 \times 1$ mm PMN-32%PT piezoelectric crystals which vibrated in the lengthwise direction and operated at about 35-45 kHz [8]. The thinness of the crystals allowed them to create a linear array with a spacing between elements which appeared to be less than $\lambda/2$. Matching layers were used over the crystals to improved performance. This array was used for guided wave excitation in a plate.

No low ultrasonic frequency arrays have been found in the literature that have combined transmission and reception. The low ultrasonic frequency air coupled transducers described above appear to have only been used for transmission and not reception. This may be related to the transducers being unsuitable for reception due to low gain and ringing effects.

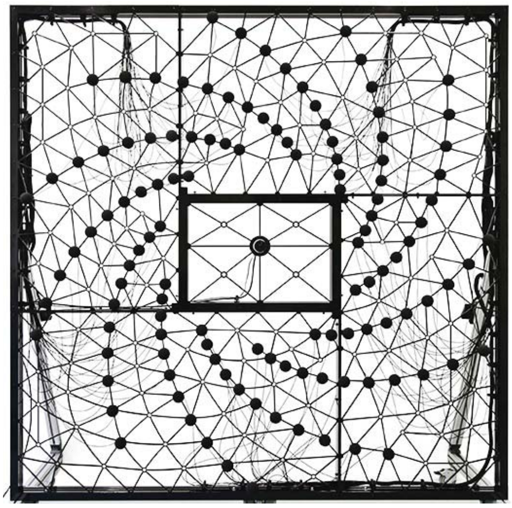

Figure 1: Photo of a commercial spiral array developed by GFaI (`www.acoustic-camera.com/`).

Most non-destructive testing transducer arrays have used transducers which are evenly spaced. However, to achieve the required resolution while avoiding aliasing, large numbers of transducers can be required. Sparse arrays have been developed that require fewer sensors while achieving similar results and have a wider bandwidth of operation. Groschup and Grosse developed a low ultrasonic frequency air couple array (receiver only and not a transmitter) for nondestructive testing of concrete structures. This array was composed of MEMS (micro-electro-mechanical system) microphones in a multi-arm spiral pattern [9]. There have also been some studies that have used a spiral configuration of transducers elements in contact ultrasound phased array probes for 3D imaging using high ultrasonic frequencies [10, 11, 12, 13, 14]. This technique has also been widely used for microphone phased arrays for audio frequencies. Examples of sparse microphone arrays are the Dougherty single arm and Underbrink multi-arm spiral arrays [15, 16, 17]. Figure 1 shows a photo of a commercial multi-arm spiral array at audio frequencies.

In this paper, we present theory and simulations for highly directional, air coupled arrays for low ultrasonic frequencies. The methodology and key parameters of interest for designing an array are briefly outlined in Section 2. In Section 3, the effect of transducer size and its potential effect on spatial aliasing are then shown using simulations. The advantages of sparse arrays compared to evenly spaced arrays are then outlined in Section 4. This section shows simulations which compare sparse arrays generated using both random placements of transducers and placement along multi-arm spirals. Finally the effect of sensor bandwidth and the effect of this on depth resolution are discussed in Section 5.

2. Array Design

Consider an array composed of sensors that are used for transmission and/or reception. The size, positions, and number of these sensors determines the operational characteristics of an array. The performance of an array (for both transmission and reception) may be simulated using beamforming. A unit magnitude ultrasonic source is defined to be located in the far-field directly in front of the array (spherical polar coordinate angle $\theta = 0$). The signal that would arrive at the sensor locations from the point source is then simulated. Far-field scanning coordinates are then calculated using unit magnitude spherical polar coordinates. These may be converted to Cartesian coordinates using

$$K_x = \sin(\theta)\ \cos(\phi) \tag{1}$$

$$K_y = \sin(\theta)\ \sin(\phi) \tag{2}$$

$$K_z = \cos(\theta). \tag{3}$$

These scan points are used to perform beamforming on the simulated signals. The resulting beamforming map may be plotted as a function of K_x and K_y. For high resolution imaging, ideally we would like the resulting beamforming map to be a single narrow beam at the source location ($\theta = 0$ or $K_x = K_y = 0$). However, the beamforming map will actually be an interference-like pattern with a main lobe and sidelobes. The spatial resolution of the array is defined to be the width of the main lobe at 3 dB down from the peak. This is referred to as the Beam Width (BW). The dynamic range is the difference in dB from the peak of the main lobe to the peak of the next highest sidelobe. This is often referred to as the Maximum Sidelobe Level (MSL).

The beam width may be approximated using

$$BW \propto \frac{R\lambda}{D} \tag{4}$$

where R is the distance from the centre of the array, λ is the wavelength, and D is the diameter of the array. This equation shows that for a set frequency and distance from the array, the resolution of the array is set by the diameter (maximum spacing between transducers) of the array [17]. Array design involves adjusting the placement of a set number of sensors to provide the desired beam width while maximising the dynamic range. This optimisation is usually achieved using a combination of far-field and near-field beamforming.

In the plots below, the beamforming maps are shown for either reception or transmission. However, if the array was to be used for both transmission and reception in pulse echo mode, the resulting beamforming maps would be the product of both the reception and transmission beamforming maps. This would result in higher dynamic ranges. It should be noted, however, that the measured performance of an actual arrays is generally lower than that of the simulations. This may be due to a range of factors. For example, the sensors will have a finite diameter while the simulations assume that each sensor is a point receiver or a point sound source for the case of transmission.

3. Sensor Diameter and Relationship with Spatial Aliasing

The minimum spacing between sensors should ideally be less than half the wave length ($\lambda/2$) of the signal being received or transmitted. If this condition is not met, spatial aliasing (multiple large sidelobes) may occur. This requirement puts an upper limit on the diameter of the sensors that should be used in an array. Figure 2 shows beamforming maps for three different arrays that are all about 80 mm in diameter but are composed of different diameter (16, 10, and 5 mm) sensors which are tightly packed in a hexagonal pattern. It can be seen that multiple grating lobes (multiple main lobes) appear for the 16 and 10 mm diameter transducers. However, for the 5 mm diameter sensor array, a single main lobe is observed and the dynamic range is about 30 dB. This is due to the fact that the spacing between transducers for this array is closer to half of the wavelength (4.3 mm for 40 kHz). This illustrates the fact that ideally one should use sensors that have a diameter that is close to or smaller than half the wavelength of the operating frequency.

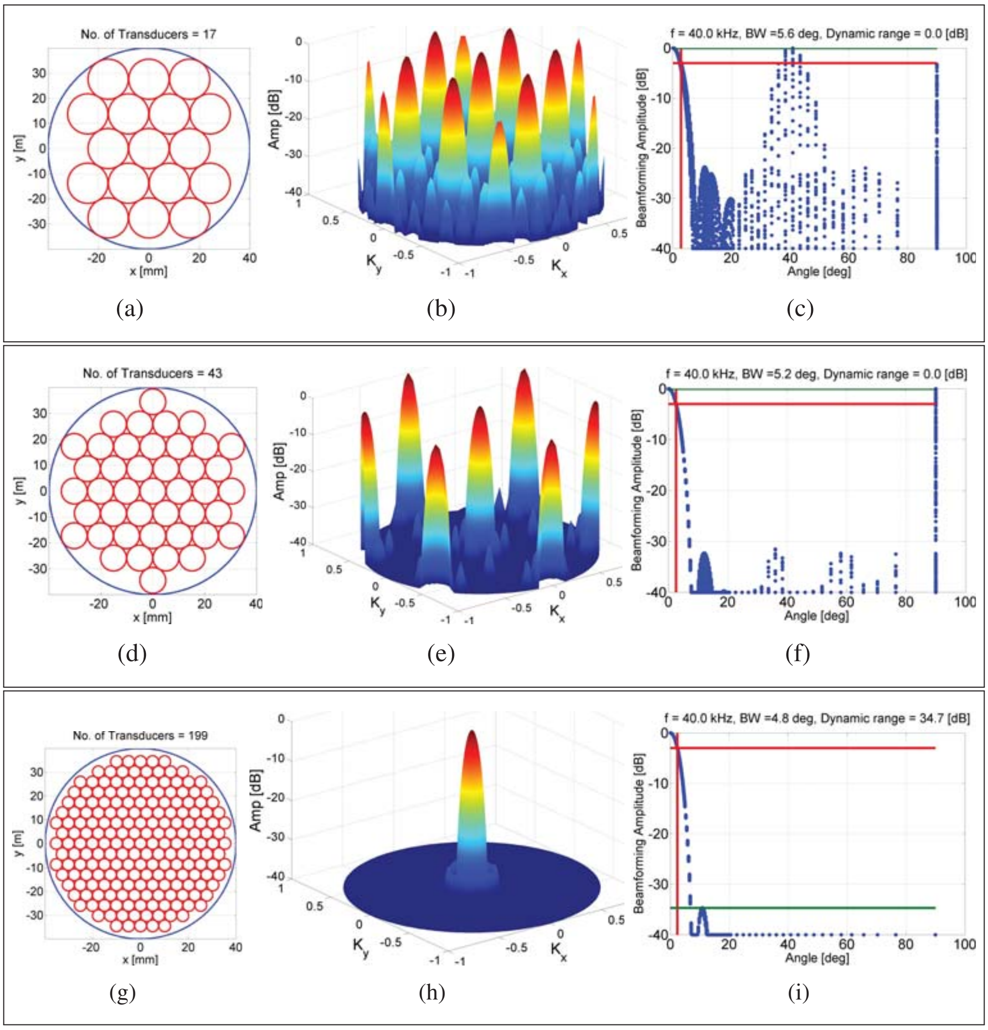

Figure 2: Plots (a), (d), and (g) show three arrays composed of respectively 16 mm, 10 mm, and 5 mm transducers packed in a hexagonal shape. Plots (b), (e), and (h) respectively show simulated 40 kHz far-field beamforming maps for these arrays. (Note that $K_x = \sin(\theta)\ \cos(\phi)$ and $X_y = \sin(\theta)\ \sin(\phi)$ where θ and ϕ are spherical polar coordinate angles.) Plots (c), (f), and (i) show the beamforming maps as a function of the spherical polar coordinate angle θ. The measurement of the beam widths and dynamic range for these beamforming maps are shown in this plot.

4. Sparse Arrays

NDT arrays generally use a constant spacing between sensors. This may take the form of a grid or hexagonal placement. However, it has been shown in the previous sections that to provide a desired resolution, the array diameter must have a minimum diameter. Also, to avoid aliasing, the minimum spacing between sensors needs to be less than a set value. This can mean that using a constant

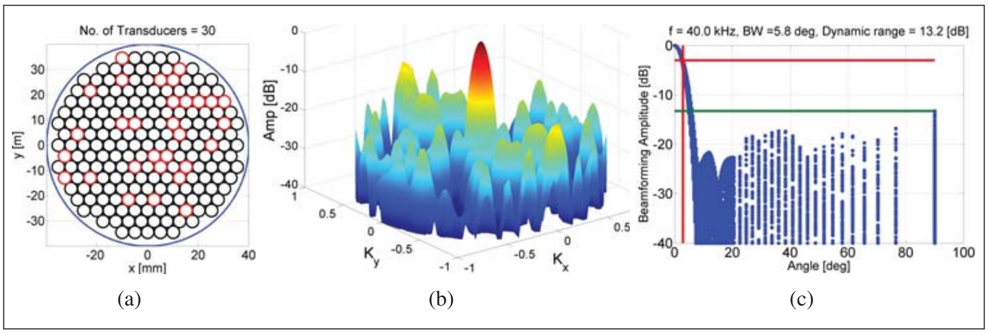

Figure 3: Plot (a) shows in red 30 sensor locations which were chosen at random from the 199 possible sensor locations shown in Figure 2(g). Plot (b) shows the simulated 40 kHz far-field beamforming map obtained for this array in Cartesian coordinates while plot (c) shows this map as a function of spherical polar coordinate angle θ.

.

spacing between sensors results in a large number of sensors being required. However, this may be undesirable due to cost and construction time. Also, these regular spaced arrays have redundancy. Refer to reference [17] for more information on this topic. Sparse array designs have, therefore, been developed that are non-redundant and, therefore, require much less sensors.

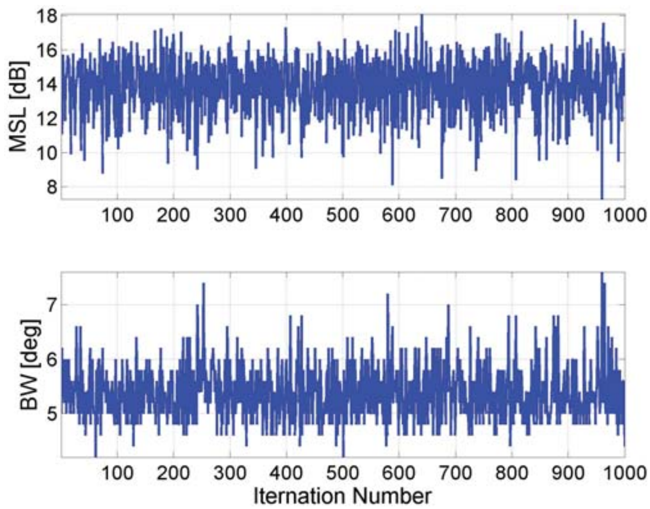

Figure 4: Simulated 40 kHz beamforming dynamic range (MSL) and beam width (BW) for 1000 different arrays generated by randomly choosing 30 sensor locations picked from the 199 sensor locations shown in Figure 2(g).

One example of a sparse array is a random array. Figure 3 shows an example simulation where 30 transducer positions were chosen at random from the 199 possible transducer locations shown in Figure 2(g). It can be seen that the resulting 40 kHz beamforming map does not show any grating lobes. It has a similar beam width compared to the array shown Figure 2(g). However, it has a reduced dynamic range compared to the tightly packed array. This simulation was repeated 1000 times to get an indication of the dynamic range and beam widths that could be achieved using this random array technique, see Figure 4. It can be seen that the beam width varied and a maximum of 18 dB dynamic range was achieved. This random method may be able to be improved by using a probability distribution.

Rather than using random placement of sensors, an alternative technique is to use a specific function that guaranties non-redundancy. One example is the multi-arm spiral similar to that shown in Figure 1. Simulations for 40 kHz were performed for multi-arm spiral arrays with 29 sensors within the same 80 mm array diameter. Figure 5 shows an example of the beam pattern that can be achieved using this technique. It can be seen that a dynamic range of 21.6 dB was achieved using this tech-

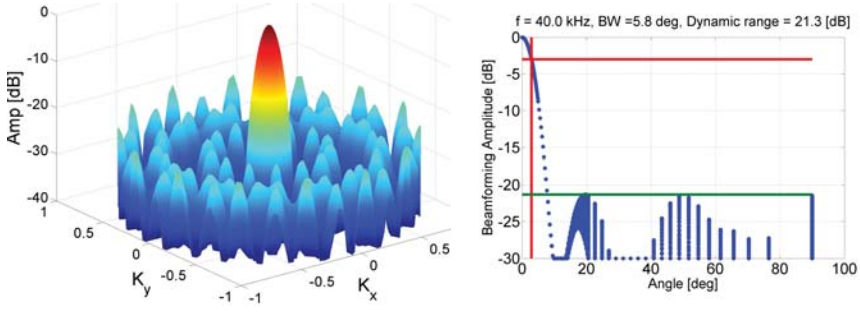

(a) (b)

Figure 5: Plot (a) shows the simulated 40 kHz far-field beamforming map obtained for a 29 sensors which are 5 mm in diameter array and arranged in a 80 mm diameter multi-arm spiral array. Plot (b) shows the map as a function of spherical polar coordinate angle θ and shows the measured beam width and dynamic range.

nique. Figure 6 shows the beam width and dynamic range that was obtained for about 320 different multi-arm spiral arrays obtained by changing the curvature of the spirals while keeping the diameter under 80 mm in diameter. It can be seen that the beam width is very constant for all the arrays, which was in contrast to the random array. Also, the dynamic range was in general better than that obtained using the random array. However, it can be seen that this is not always the case and some maximisation is required to an achieve optimal array design using this method. An advantage of using spiral arrays is that they have a very wide frequency bandwidth of operation compared to a grid array. The simulated spiral array have an operational frequency of about 25 to 65 kHz.

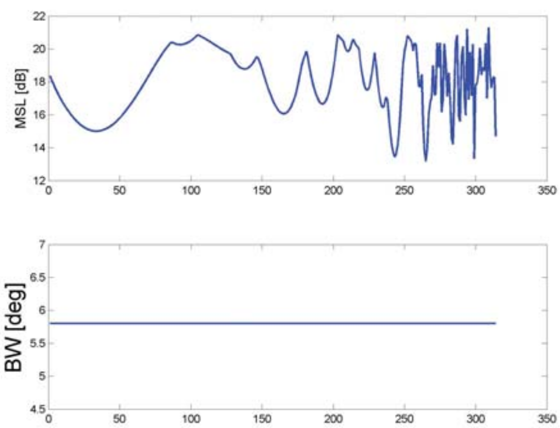

Figure 6: Simulated dynamic range (MSL) and beam width (BW) for about 320 different multi-arm spiral arrays generated by iteratively varying the curvature if the spirals on which the transducer were placed.

5. Depth Resolution of an Array

Depth resolution is challenging for low ultrasonic frequency arrays due to the longer wavelengths used. The choose of sensors is, therefore, important to enhance the depth resolution. As shown above, the diameter of the sensor can determine if aliasing (grating lobes) occur. However, another feature that should be considered is how much the sensor rings after experiencing a disturbance (a signal is transmitted or received). Many ultrasonic sensors have narrow frequency bandwidths. This can be beneficial for minimising noise. However, the narrower the bandwidth is, the more resonant the transducer becomes. This can result in the sensor ringing which has a detrimental effect on the temporal (depth) resolution of the array. For example, a sensor with a central frequency of 40 kHz will tend to ring at this frequency and the output signal will generally have a longer duration than the excitation signal. This factor needs to be considered when choosing a suitable sensor for both transmission and for reception.

6. Conclusion

Air coupled ultrasonic transducers may be used for non-contact non-destructive evaluation of the properties of materials or structures. These transducers should have highly directional transmit and receive beams and good depth resolution. However, air coupled transducers have poor resolution at low ultrasonic frequencies due to wide beam widths and long duration transmit pulses. In this paper, we presented theory and simulations which showed how low ultrasonic frequency air coupled arrays may be developed that have highly directional transmit and receive beams and improved depth resolution for frequencies from about 25-65 kHz.

REFERENCES

1. M. C. Remillieux, B. E. Anderson, T. J. Ulrich, P.-Y. Le Bas, M. Haberman, and J. Zhu, "Review of air-coupled transduction for nondestructive testing and evaluation," *Acoust. Today*, vol. 10, no. 3, pp. 36–45, 2014.

2. D. Chimenti, "Review of air-coupled ultrasonic materials characterization," *Ultrasonics*, vol. 54, no. 7, pp. 1804–1816, 2014.

3. F. M. de Espinosa, J. Chavez, Y. Yañez, J. Salazar, A. Turo, F. Chinchurreta, and M. Garcia-Hernandez, "Air-coupled piezoelectric array transducers for NDT applications," in *16th World conference on non-destructive testing*, Citeseer, 2004.

4. A. Octavio, R. L. O'Leary, S. M. Whiteley, Ó. Martínez-Graullera, C. J. Martín-Arguedas, L. Gómez-Ullate, and F. M. de Espinosa, "Air-coupled linear and sparse cMUT array manufactured using MUMPs process," *Microsystem technologies*, vol. 17, no. 10-11, p. 1635, 2011.

5. F. Blum, J. Jarzynski, and L. J. Jacobs, "A focused two-dimensional air-coupled ultrasonic array for non-contact generation," *NDT & E International*, vol. 38, no. 8, pp. 634–642, 2005.

6. E. Konetzke, M. Rutsch, M. Hoffmann, A. Unger, R. Golinske, D. Killat, S. N. Ramadas, S. Dixon, and M. Kupnik, "Phased array transducer for emitting 40-kHz air-coupled ultrasound without grating lobes," in *Ultrasonics Symposium (IUS), 2015 IEEE International*, pp. 1–4, IEEE, 2015.

7. A. I. Korobov, M. Y. Izosimova, and S. A. Toschov, "Development of ultrasound focusing discrete array for air-coupled ultrasound generation," *Physics Procedia*, vol. 3, no. 1, pp. 201–207, 2010.

8. R. J. Kazys, R. Sliteris, and J. Sestoke, "Air-coupled low frequency ultrasonic transducers and arrays with PMN32%PT piezoelectric crystals," *Sensors*, vol. 17, no. 1, p. 95, 2017.

9. R. Groschup and C. U. Grosse, "Mems microphone array sensor for air-coupled impact-echo," *Sensors*, vol. 15, no. 7, pp. 14932–14945, 2015.

10. J. L. Schwartz and B. D. Steinberg, "Ultrasparse, ultrawideband arrays.," *IEEE transactions on ultrasonics, ferroelectrics, and frequency control*, vol. 45, no. 2, pp. 376–93, 1998.

11. T. S. Sumanaweera, J. Schwartz, and D. Napolitano, "A spiral 2D phased array for 3D imaging," in *Ultrasonics Symposium, 1999. Proceedings. 1999 IEEE*, vol. 2, pp. 1271–1274, IEEE, 1999.

12. O. Martinez-Graullera, C. J. Martin, G. Godoy, and L. G. Ullate, "2D array design based on fermat spiral for ultrasound imaging.," *Ultrasonics*, vol. 50, pp. 280–9, Feb 2010.

13. F. Reverdy, G. Ithurralde, and N. Dominguez, “Advanced ultrasonic 2D phased-array probes,” in *Proc. of the 18th Conf. on Non-Destructive Testing*, (Durban, South Africa), 16-20 Apr. 2012.

14. A. Ramalli, E. Boni, A. S. Savoia, and P. Tortoli, “Density-tapered spiral arrays for ultrasound 3-D imaging,” *IEEE transactions on ultrasonics, ferroelectrics, and frequency control*, vol. 62, no. 8, pp. 1580–1588, 2015.

15. R. P. Dougherty, “Spiral-shaped array for broadband imaging,” Nov. 17 1998. US Patent 5,838,284.

16. J. R. Underbrink, “Circularly symmetric, zero redundancy, planar array having broad frequency range applications,” Mar. 20 2001. US Patent 6,205,224.

17. J. R. Underbrink, “Aeroacoustic phased array testing in low speed wind tunnels,” in *Aeroacoustic measurements*, pp. 98–217, Springer, 2002.